SPE/IADC 105405

Assuring Stability in Extended-Reach Wells—Analyses, Practices, and Mitigations

Stephen M. Willson and Stephen T. Edwards, BP America Inc.; Anthony Crook and Adam Bere, Rockfield Software Ltd.; Daniel Moos and Pavel Peska, GeoMechanics Intl. Inc.; and Nigel Last, BP plc

This paper was prepared for presentation at the 2007 SPE/IADC Drilling Conference held in Amsterdam, The Netherlands, 20–22 February 2007.

Abstract

Whilst the step-out lengths of proposed ERD wells are becoming more and more challenging, wellbore stability assurance technologies - both in the pre-planning and execution phases - are developing at an equal pace. In this paper we describe several new developments in theoretical understanding and predictive capability of rock failure surrounding wells drilled at high-angle to bedding that are required to solve the problems encountered in these challenging environments. Rig-site processes for the integration of this new understanding with real-time diagnostic measurement and monitoring provide the means to deliver borehole stability assurance for ERD wells drilled in the most challenging environments.

Introduction

It has been 10 years since the temporary suspension of the extended reach drilling (ERD) program in the Niakuk field, North Slope, Alaska, due to the severe wellbore instability problems in the 8.5-in sections of successive ERD wells. The peer review[1] and studies[2,3] that were commissioned to investigate these problems highlighted the importance of integrating, in a holistic way, results of wellbore stability prediction, drilling fluid optimization, hydraulics and cuttings transport, operational practices and PWD tool utilization.

Since the Wytch Farm, UK and Niakuk, Alaska, ERD well drilling campaigns in the mid-'90s, there has been a steady progression in the vertical depth and horizontal departure length of ERD wells drilled world wide (Figure 1)[4]. Wells with horizontal departures in excess of 40,000 feet (12 km) at vertical depths of less than 10,000 feet (3 km) are now being actively considered as a viable way of accessing satellite reserves from existing facilities or, in the case of environmentally-sensitive arctic environments, to develop offshore fields from onshore locations.

A review of the recent SPE conference literature reveals that the challenges of ERD well feasibility planning and execution identified at Niakuk persist to the present day. Notable case history summaries have been presented by ExxonMobil for their Sakhalin-1 development in the Russian Far East. Here the offshore Chayvo field reservoirs are being accessed from an onshore location using ERD wells with reaches of 9 to 11 km[5,6]. In the Norwegian part of the North Sea, ExxonMobil again are using ERD drilling technology to access multiple independent reservoirs from their Ringhorn development, requiring well departures of up to 8 km[7]. Elsewhere in the Norwegian sector, Statoil have successfully drilled ERD wells with up to 7593 m (24911 ft) departure from their Visund platform; a record from a floating installation[8,9]. The reader is particularly directed to these papers, plus their associated references and bibliography, for a recent compilation and discussion of drilling engineering aspects of ERD well construction. In the rest of this paper, the authors will focus on the wellbore stability aspects of ERD wells. Particularly, new understanding and predictive capability for assessing instability in wells drilled at high angles to bedding are presented. Real-time drilling monitoring and operational practices are discussed, as are approaches that can be applied to minimize the risk of incurring wellbore instability problems in extended reach and high-angle wells.

Wellbore instability in ERD wells – what's different about it?

One can legitimately question whether wellbore instability in ERD wells differs significantly from instability occurring in near-vertical wells and in high-angle wells of lesser departure. It is the authors' opinion that there are differences in assessing and addressing wellbore instability in ERD wells. The additional considerations are more subtle in relation to conventional high-angle wells, but extra assurance steps are considered necessary. The list below summarizes particular issues that should be addressed when planning ERD wells.

Well depth relative to ground elevation or seabed

Significant variations in seabed depth or ground elevation may occur along the ERD well path. Simple 1-dimensional assessments of pore pressure, fracture gradient and in-situ stresses will not apply in these cases. For example, changes in water depth in excess of 2000 feet can occur over lateral distances of about 2 miles in the vicinity of the Sigsbee Escarpment in the deepwater Gulf of Mexico (GoM). The deepwater GoM fields Mad Dog and Atlantis both underlie the

Sigsbee Escarpment. Though the principal production facilities will be located on top of the escarpment in shallower water (ca. 4420 feet water depth), some extended reach wells will be drilled into areas of the field lying in deeper water (up to 6500 feet water depth).

One-dimensional predictions of pore pressure and fracture gradient are inappropriate in the design of such wells. To accurately predict pore pressures and fracture gradients, the varying water depth has to be taken into consideration. The lower fracture gradient (relative to that for a shallower water vertical well profile) existing over the long tangent section of extended reach wells drilled from the escarpment to access deeper water reserves is an important aspect in the well design. In this case, an extra casing string is usually required in the tangent section – see, for example, deepwater drilling experiences in the GoM and Campos Basin, offshore Brazil[10,11].

Additionally, the presence of the free surface of the escarpment can reduce the magnitude of the near-surface fracture gradient below that expected for intra-basin locations. Failure to recognize this effect in the well planning stage could lead to circulation losses in the top-hole sections of the well. Where such problems are of particular concern, 2D or 3D finite element predictions of stress states may be warranted.

Well trajectory in relationship to bedding

Extended reach wells – particularly their tangent and often near-horizontal reservoir sections – may be drilled at a very shallow angle to bedding. This can give rise to additional mechanisms of instability that cannot be simply solved by increasing mud weight. In their seminal paper, Økland and Cook[12] provided the earliest clear picture of the influence of bedding instability effects on borehole trajectories that are drilled nearly parallel to bedding (Figure 2). The buckling instability of delaminated shale layers can be clearly seen in this photomontage. The 'blocky' or 'tabular' cavings produced by this mode of instability are a characteristic of bedding-parallel instability in the field[13,14] – see Figure 3. Økland and Cook[12] concluded that this failure mode was prone to occur in wells drilled within 15° of the bedding parallel direction. Further discussion and analysis of this is presented later in this paper.

Well trajectory in relationship to faults

It is common to use ERD wells to access satellite reserves distant from the main development hydrocarbon accumulations. These well paths invariably require crossing faults, sometimes at unfavorable orientations. The risk of losses and instability associated with fault zones should be assessed in the planning of any ERD well drilling campaign.

Recommended practices for drilling faults covers a very wide range of issues that are beyond the scope of this paper. Only a few of the more pertinent topics are included here. From a drilling perspective, well trajectories that cross major faults at an oblique angle have a high risk of suffering losses or instability, as the fault plane can be exposed for a significant distance along the well path.

The fault may be thought as comprising two zones – a central comminuted fault 'core' zone, and a wider zone on either side of the fault core that can be mechanically damaged[15]. The extent of the damage zone depends upon the timing of the fault movement relative to the lithification state of the surrounding rocks. Geologically recent fault movement in already lithified rocks poses the greatest risk for incurring borehole instability in the brecciated 'rubble' that may surround the fault[16].

Stress states may vary in the vicinity of faults – both in terms of stress direction and minimum horizontal stress magnitude. Figure 4 shows the reorientation of breakouts, as seen in an Ultrasonic Borehole Image (UBI) log, in the vicinity of a fault zone[17]. Depending upon the magnitude of stresses acting on the fault, the fault zone itself might be permeable and a conduit for massive losses while drilling[18]. Figure 5 shows the close correspondence between fault crossings and the occurrence of losses in high-angle wells drilled on the Prudhoe Bay Field, Alaska[19]. It is considered important to assess the state of stress acting on faults and the potential for losses when planning ERD wells as these losses can occur at mud weights lower than those needed to maintain stability in the surrounding formations away from the fault-affected zone.

Wellbore instability in shallow hole sections

There is a tendency to aggressively build angle in the upper hole sections of ERD wells, particularly those accessing reservoirs shallower than 10,000 ft vertical depth. This can lead to instability in these weak sediments as low fracture gradients preclude the use of high mud weights. Willson et al[10] provided a good example of this at the Pompano field.

Here the MC 29 TB-9 well was designed as an 11,780 feet TVD / 20,454 feet MD / 12,000 foot step-out extended reach well. The planned deviation was aggressive to achieve the desired step-out, kicking-off below the 20-in. shoe and deviating up to 68º in the 17½-in. hole section. This deviation was greater than in other wells, where the 17½-in. hole section had previously been built to a maximum of 35º only. The planned 68º tangent section was maintained in the 12¼-in. hole, after which the deviation was dropped to 40º though the reservoir section.

As predicted, the top-hole sections of TB-09 did prove challenging from a wellbore stability standpoint. Figure 6 summarizes the predicted minimum mud weight, pore pressure and fracture gradient, as well as the mud weight used to drill the top-hole sections of this well. Of significance, the predicted mud weight in the build to 68º section and top of the tangent section is between 1.0 ppg to 2.0 ppg higher than the pore pressure. This is in contrast to the more nominal mud overbalances (0.3 to 0.6 ppg above pore pressure) needed when drilling near-vertical wells at these depths. This is due to the low rate of strength increase with depth relative to the divergence between overburden and horizontal stress; i.e. additional mud weight is needed to achieve stable wellbores at high deviations in shallow sediments. This is a portion of the well that might traditionally be given less attention in conventional wells, but which needs careful consideration in ERD well planning.

Hole section lengths tend to be longer

In order to maintain a conventional (e.g. 8.5-in) hole size through the reservoir interval, hole sections through the

overburden tend to be longer than in vertical wells drilled to a similar vertical depth. The time that the open borehole will be exposed to the drilling fluid and to drilling events will be longer, relative to conventional wells. This increases the susceptibility for a number of time-dependent effects to occur.

Longer hole sections expose the formation to more cycles of pressure variation – when making connections or from drill-pipe contact with the borehole wall. This can reduce the strength of the formation as a consequence of fatigue-type mechanisms[20]. Figure 7 shows cyclic loading tests run on twinned samples of Pierre 1 Shale. The axial strain rate was 1×10^{-6} sec^{-1} (i.e. slow, allowing some drainage, but not fully drained). The unconfined compressive strength (UCS) test (red curves in Fig. 7), loaded monotonically to failure, reached a peak strength of 1683 psi. The second UCS test was stressed to 1250 psi – approximately 75% of the peak failure stress - and was then subjected to stress cycles of ±250 psi around this mean (green curves in Fig. 7). The sample failed at 1387 psi on the 80th load cycle of this magnitude. This represents a strength degradation with repeated loading of approximately 20%.

The third test was stressed to 1000 psi - approximately 60% of the peak failure stress - and was then subjected to similar stress cycles of ±250 psi around this mean. This sample did not fail, even after 200 applications of cycling. (This test took over 7 days to complete). A subsequent UCS test ran on this sample gave a failure stress of 1730 psi – essentially unchanged from the 'uncycled' value.

It is conventional practice in wellbore stability prediction to allow a certain amount of circumferential failure around the borehole[10,17]. Portions of the borehole wall, therefore, will be stressed to relatively high levels compared to the formation compressive strength. As a consequence of this, some degradation of strength may be expected when drilling ERD wells. This should be taken into account in stability predictions. For example, at a vertical depth of 12,500 feet, a 500 psi pressure excursion (±250 psi) would be equivalent to a 0.77 ppg pressure fluctuation – a not unreasonable change between equivalent circulating density (ECD) and equivalent static density (ESD). If drilling a 7200 feet-long open hole section at this depth, the shallowest exposed formation at the previous casing shoe would be subjected to approximately 80 stress cycles (ECD - ESD) culminating from connections using 90 feet-long stands of drill pipe. Strength degradation should, therefore, be considered as a potential destabilizing mechanism along with other time-dependent effects when designing challenging ERD wells.

The potential for chemo-mechanical interactions between the exposed formation and water-based drilling fluids has long been recognized[21]. However, of significance to ERD well planning are the recent observations by Rojas et al[22] that adverse osmotic potentials can occur even with the use of synthetic oil-based drilling fluids if the activities are not balanced. Where the drilling fluid has a high salinity (i.e. low activity) relative to the adjacent formation, fluid will be pulled from the formation into the drilling fluid. The rate at which this occurs depends upon the salinity difference, the permeability of the shale and the amount of mud overbalance. The process of osmotic-driven fluid exchange can occur in both synthetic oil-based drilling fluids, as well as in water-based fluids. This is because osmotic flows are created in response to the electrical potential existing between the water phases; contact of the phases is not required for this to occur.

Figure 8 shows the extent of desiccation cracking occurring in a GoM shale sample after exposure to synthetic drilling fluids with different water-phase salinities. (The water / oil ratio was 25 / 75 in each fluid used)[22]. The salinity of the shale is approximately equivalent to 17% by volume $CaCl_2$. When exposed to drilling fluids with a very saline water phase, water is pulled from the formation shale into the drilling fluid. This causes shrinking and cracking of the shale over time, as is clearly seen in Fig. 8. Cracking is not seen in shales with a more balanced activity. The cracking seen when using the more saline drilling fluids is a potential cause of time-delayed instability.

The extent to which time-dependent effects can destabilize a wellbore is clearly shown in Figure 9. Here azimuthal density image logs collected at various times during and after drilling are compared for a single depth in a recently drilled ERD well in the North Sea. Here high density values are shown in dark brown colors. The tool images broken-out portions of borehole as having a lower density value; these are shown in the pale yellow colors. The severely enlarged regions of the borehole are colored white. Fig. 9 shows the borehole was in excellent condition when it was logged using logging-while-drilling (LWD) tools. A subsequent LWD image was collected while reaming the borehole several hours after first drilling. Some minor breakout is seen to form some 8 hours after first drilling. As the well was drilled further, hole conditions deteriorated over time. Mechanical problems with the drill-rig also delayed completing this hole section. LWD logs taken while reaming 5 days and 9 days respectively after first drilling the section show rapidly worsening hole conditions. This section was eventually abandoned after the last back-reaming run, and the well was sidetracked. The mechanisms contributing to this mode of instability, and predictive approaches to this problem, are described in the following section.

Recent advances in wellbore stability prediction in high-angle ERD wells

Borehole failure in rocks with anisotropic strength

Conventional approaches to predict wellbore stability for routine applications have been covered extensively in the published literature – see for example Zoback[17]. When drilling high-angle wells, additional mechanisms of failure – as illustrated in Fig. 2 – can become dominant. In the recent Shenzie field development in the deepwater Gulf of Mexico it was noted that "While drilling the first wells, it was observed that the borehole instabilities were more severe when drilling down dip at low angles-of-attack to bedding, but almost non-existent when drilling up-dip at angles nearly perpendicular to the bedding planes"[23]. This observation echoes those of other studies undertaken a decade earlier[24,25]. This mode of instability occurs in rocks that are anisotropic in their strength characteristics[25]. Conventional wellbore stability prediction approaches typically assume the rock to possess isotropic strength; i.e. when a sample of the rock is loaded in a particular direction, the orientation of the failure plane and the

ultimate strength of the rock are independent of the orientation of the bedding planes. However, when anisotropic rocks are loaded to failure, the failure plane is dictated by the orientation of the bedding, and the ultimate strength can be significantly reduced. Numerical orthotropic strength models have been developed to reproduce this effect[26].

The anisotropic nature of shales is well known experimentally[27,28]. These data show a pronounced variation of formation strength as a function of the angle, θ, between the direction of the axial stress and the normal to the plane of weakness (Figure 10). Formation strength is highest at orientations perpendicular to bedding (θ = 0°); lowest when θ = 60°; and has an intermediate value when tested parallel to bedding (θ = 90°). After normalizing the formation strengths relative to the strength perpendicular to bedding for three shales – Tournemire shale[27], a "siltshale"[28] and a "mudshale"[28] (Fig. 10) – a similar variation in strength with angle to bedding is apparent, with a strength minimum at θ = 60°. Overburden shales encountered when drilling at the Niakuk field[2] exhibit similar strength behavior. In these fissile shales, the strength at the most unfavorable orientation to bedding (θ = 60°) is only 10% to 40% of that measured perpendicular to bedding. Even when tested parallel to bedding, strengths can be reduced to 40% to 90% of that measured perpendicular to bedding. This variation is of importance to wellbore stability, as the stress concentration existing around a borehole drilled in a near-parallel to bedding trajectory interacts with formation of different intrinsic strength as the stress orientation changes. This is shown schematically in Figure 11. In the horizontal borehole shown, the maximum stress concentration (for an assumed normal faulting condition) acts at the 3 o'clock and 9 o'clock positions around the borehole. Here the strength normal to bedding is the greatest. At approximately the 2 o'clock and 10 o'clock positions the stress concentration acts on the minimum rock strength. At the 12 o'clock and 6 o'clock positions, the stress concentration is at its least compressive magnitude, and the rock strength has an intermediate value. Depending on the relative magnitudes of anisotropic rock strength and stress concentration, breakouts may occur at "unexpected" positions around the borehole. If the strength perpendicular to bedding is sufficiently large, breakout formation on the sides of the borehole may be suppressed (as seen in Fig. 2). If the minimum formation strength is very low, breakouts may form on the upper sides of the borehole (failed material at the 4 o'clock and 8 o'clock positions may remain in place by the action of gravity), so producing a "square" breakout shape[23]. Rock failure at the 2, 4, 8 and 10 o'clock positions around the borehole can also trigger additional delamination of the rock, resulting in the "roof collapse" style of failure shown in Fig. 2. Depending upon the stiffness and strength of the formation, this roof collapse failure may be exaggerated by the buckling instability of individual laminae if sufficiently thin[29].

Orthotropic strength vs. single plane of weakness models of shale failure

Fig. 10 shows that the Pierre I Shale strength variation (BP-proprietary data) is different to that exhibited by the other shales. In contrast to a strength reduction seen at relatively small orientations to bedding, the Pierre I Shale exhibits an almost constant strength until close to a bedding orientation of θ = 45°, where a lower strength of approximately 60% of that perpendicular and parallel to bedding occurs.

This strength variation with respect to bedding is not orthotropic, as in the case of the other shales in Fig. 10, but is a combination of uniform strength supplemented by failure along a discrete bedding plane of a specific orientation[30,31]. Such a failure mode can be characterized by a "single plane of weakness" model[25]. Here the plane of weakness is characterized as having Mohr failure properties (cohesion, c, and angle of friction, ϕ′) distinct from those of the intact rock. Figure 12 shows a comparison between the predicted failure strength of Pierre I Shale in unconfined compression assuming both an orthotropic strength model and a single plane of weakness model. In this instance the bedding plane was assigned strength properties of 628 psi cohesion and a friction angle of 0°. This results in the minimum strength occurring at an orientation of (45 + ϕ′/2)°; i.e. at 45°. This predicts the correct experimental data minimum, occurring at 45°, by virtue of the 0° angle of friction appropriate to the relatively fast loading rate imposed in the experiments giving rise to 'undrained' conditions[32]. Samples tested at a slower rate, allowing dissipation of generated pore pressure, would be expected to exhibit frictional behavior, thus moving the bedding orientation at which the minimum strength occurs.

Wellbore stability prediction using orthotropic strength and single plane of weakness models

Wellbore stability predictions may be made utilizing assumptions of either orthotropic strength or a single plane of weakness. Predictions of this kind are recommended whenever the well trajectory approaches to within 30° of the bedding-parallel direction. Experience shows that intersections oriented more normal to bedding are unlikely to result in significant additional instability, even in the presence of weak bedding planes. Remember, however, that in complex geology with steeply-dipping beds, even modestly-deviated wells might be drilled near to a bedding-parallel orientation[25].

Both numerical and analytical approaches may be utilized with orthotropic strength or single plane of weakness models[e.g.26, 33, 23]. When considering orthotropic strength, the variation with respect to bedding may be defined empirically (e.g. by a regression curve-fit analysis to the experimental data), or via an analytic expression. To accommodate altered formation strength relative to bedding, an amended formulation is proposed for unconfined strength. Adopting the convention of Niandou et al[27], the level of strength orthotropy may be characterized by two constants:

$$k_1 = q_{//}/q_{\perp} \quad \text{and} \quad k_2 = UCS_{min}/UCS_{max} \qquad \text{Eq. (1)}$$

In the above, $q_{//}$ is the strength with the bedding parallel to the sample axis; $q_{\perp}$ is the strength with the bedding perpendicular to the sample axis; UCS_{max} is the maximum strength at any orientation; and UCS_{min} is the minimum strength at any orientation. To derive a smoothly-varying strength profile with bedding orientation, the following assumptions are made:

- $q_{\perp}$, the strength perpendicular to bedding, equals the maximum strength, UCS_{max}.
- UCS_{min}, the minimum strength occurs at an orientation of 45° to bedding. This is a reasonable assumption for shales undergoing relatively rapid failure (i.e. at undrained, or at least, partially drained conditions) as the mobilized angle of friction, ϕ', is very small (typically <10°). In this situation, the failure along the critical shear plane at angle $(45 + \phi'/2)$ is approximately equal to 45°.

Based on these assumptions, the following strength variation is proposed, relative to the stress concentration orientation to bedding, θ. Note that θ = 0° represents loading perpendicular to bedding and θ = 90° represents loading parallel to bedding:

$$UCS_{\theta} = UCS_{max} \times (\cos\theta + k_1 \sin\theta).(1 - \sin\theta\cos\theta).\left(1 - 2\sin\theta\cos\theta \times \left(1 - \frac{4k_2}{\sqrt{2}(1+k_1)}\right)\right) \quad \text{..... Eq. (2)}$$

Figure 13 compares the orthotropic strength variation with k_1 = 0.6 and k_2 = 0.2 with the experimental data from the Kingak and HRZ shales[2]. The form of the variation is reasonable, though the experimental strength minimum at θ = 60° is not replicated due to the assumptions inherent in the derivation of Eq. (2). This discrepancy is not considered to be too detrimental, as at orientations approaching the bedding-parallel direction (45° ≤ θ ≤ 90°), the analytic expression matches the experimental data with acceptable accuracy.

Comparison between numerical and analytical simulations of borehole failure - stability of horizontal wells

Problem definition. For the purposes of this paper, the stability of horizontal wells is easiest to model as the borehole is aligned with the principal stress directions. This permits a two-dimensional (2D) analysis to be performed. With the additional assumption of horizontal bedding, the effects of varying formation strength can be easily assessed using both the orthotropic and plane-of-weakness models. The following scenario has been used in this comparison:

Vertical stress, S_v	= 10,230 psi
Minimum horizontal stress, S_{hmin}	= 8,000 psi
Maximum horizontal stress, S_{Hmax}	= 9,000 psi
Pore pressure, P_p	= 6,000 psi
Drilling mud overbalance	= 800 psi
Well direction	= aligned with S_{Hmax}

The strength properties assigned to the formation assume a 'perpendicular to bedding' unconfined compressive strength (UCS_{max}) of 2130 psi with an angle of friction of 25º (tan 25º = 0.4663). In the orthotropic model, the lowest strength, UCS_{min}, was taken to be 25% of the formation strength measured perpendicular to bedding.

In the weak plane model of this formation, the discrete weak plane properties have been chosen to provide a strength equivalent to 28% of the UCS measured perpendicular to bedding. Here a lower friction angle is assumed, giving the cohesion on the plane of weakness, c = 180 psi and ϕ' = 19º (tan 19º = 0.3443). The stability analyses have assumed a horizontal well being drilled in the least stable trajectory (towards S_{Hmax}). A mud overbalance of 800 psi is assumed in all analyses. The numerical analyses have considered an orthotropic continuum, and a laminated sequence with discrete layering incorporating a 0.88-in. bed spacing. In all cases an 8½-in. diameter borehole is assumed.

Results of analyses. The numerical results using an isotropic strength (i.e. no variation with bedding) are shown in Figure 14. Equivalent plastic strain, ε_p, is used as a proxy for damage. The creation of breakouts is very evident around the borehole circumference. The 'quarter-symmetry' damage angle, ψ, equivalent to one-half the breakout width, wBO, predicted by the analytical simulations, is superimposed on the plotted results. The numerical predictions show clearly the additional instability induced by the bedding-orientation sensitive orthotropic model. The quarter-symmetry damage angle, ψ, increases from 32° for the case of isotropic strength, to 80° when considering the orthotropic strength variation described above.

The results of the analytical predictions of breakout extent are shown in Figure 15. For the isotropic (uniform) rock strength assumption, a breakout width, wBO, of 69º (i.e. ψ = 34½º) is predicted using the Modified Lade Criterion. This is in excellent agreement with the equivalent wBO angle of 64° predicted by the numerical model which uses a comparable "soft rock" orthotropic strength model[26]. Extending the analytical model to consider orthotropic strength, as defined by Eq. 2, the breakout width is extended to 120°. This compares somewhat less favorably with the numerical prediction of 160° (i.e. ψ = 80º), although this discrepancy can be explained by the stress redistribution that occurs once portions of the near-wellbore region have been stressed to a point that exceeds the peak strength. (The 'load shedding', which is not accounted for in the analytical model, causes additional failure in the numerical model as a proportion of the stress acting on the failed material is transferred to other regions surrounding the borehole). From a practical point of view, however, the predicted breakouts by both the numerical and analytic orthotropic models would be considered too severe for trouble-free drilling operations to be possible.

Numerical predictions were also made using a discrete plane-of-weakness model. The results of these predictions are shown in Figure 16. Here the spacing of the bedding (0.88-in spacing in this analysis) clearly influences the resulting distribution of plastic strain, as well as the yes/no bedding slip indicator. In this analysis the extent of borehole failure in the quarter-symmetry model is about 60°, giving rise to a full breakout width of 120°.

The equivalent analytical model predictions of borehole failure using a single plane of weakness model are presented in Figure 17. Here the breakout width is increased from 69º for the case of isotropic rock to 135º for the rock model used. The analytical result is in broad agreement with the comparable numerical prediction; in the analytical model wBO = 135° compared with 120° in the numerical prediction. For this example the analytical single plane of weakness

model also agrees with the analytical model incorporating orthotropic strength (wBO = 135° in the single plane of weakness model compared with 120° in the analytical orthotropic strength analysis). These results suggest that it is in fact possible to assess wellbore instability risks when drilling at high angles to bedding, provided bedding plane failure effects are introduced to the analysis, and that a reasonable strength reduction is modeled.

Real-time technologies & practices to assure wellbore stability in high-angle wells

The previous section has described some recent advances in wellbore stability prediction that are particularly relevant to the design of ERD wells. In parallel with these advances in prediction capability, improvements have also been made in real-time drilling monitoring and diagnosis. The use of LWD sonic and resistivity logs to update predictions of pore pressure while the well is being drilled is now commonplace; e.g. References 34 and 35. Since the early application of "high-tech" real-time wellbore stability prediction services in the late 1990s[13], this technique too is becoming more widely implemented[36,37,38].

The current industry common practice when conducting a wellbore stability prediction is to use caliper log information and borehole images to constrain the in-situ stress state[17,39]. The reader is referred to these two referenced works for in-depth discussion of how this methodology is typically implemented. In short, known or inferred information regarding the overburden; the minimum horizontal stress or fracture gradient; pore pressure; and drilling mud hydrostatic pressure, are supplemented with derived properties for formation strength (often via velocity correlations), to perform a back-analysis of observed borehole quality in order to generate a self-consistent explanation of observed events. The models are self-consistent in that different derived parameter values may be obtained depending on certain assumptions made in the analysis (most notably the rock failure criterion[17]). However, provided the same assumptions are used consistently in the back-analysis of events and the forward-prediction of new well conditions (e.g. changed trajectory or mud weight), then the predicted mud weights can be used with some confidence for other wells or sidetracks in the field in question – see, for example, References 2, 10 and 25 for field case-history applications of wellbore stability prediction.

The key piece of information in making reliable wellbore stability predictions is having some form of borehole quality indicator upon which to calibrate or predict unknown parameter values – most notably the magnitude and, oftentimes, the direction of the maximum horizontal stress. The best hole quality information typically available in oil-industry wells is in the form of borehole image logs, such as that shown in Fig. 4. The widths of the breakouts (the dark brown longitudinal smudges) may be directly scaled from these images for use in back-analyses of the conditions causing such instability.

The main technology enabler, developed in recent years, has been the ability to transmit down-sampled (albeit they are consequently coarser) images recorded by LWD "image log" tools in real-time. (Previously, these tools were only available as wire-line deployed versions, or without real-time telemetry capability). The availability of such information in real-time at the drill-site, or transmitted from there also in real-time via the internet, has enabled a far more advanced diagnosis of well failure modes than was possible in the past. Bratton et al[40] present an excellent overview of the failure modes, plus associated resistivity-at-the-bit ("RAB-tool") images, that might be seen in real-time image logs in unstable boreholes.

While the RAB-tool, and other vendor-specific counterparts, are proper image logging tools designed for real-time use, it has been the recent adoption of "pseudo" image logs that has really permitted the widespread possibility of undertaking real-time wellbore stability prediction[16]. Fig. 9 presents an excellent example of such a pseudo image log.

Formation imaging tools are now available that can provide high-resolution azimuthal resistivity or density data while drilling. Coupled with improved mud-pulse telemetry capabilities, the LWD data may be transmitted to the drill site to provide information on formation geology (e.g. layering and dip, fault location and orientation) to aid geosteering the well to its desired bottomhole location[41]. In these tools, resistivity or density measurements are made using high-resolution sensors. During tool rotation and whilst drilling ahead, the measured resistivity or density data are binned into typically 56- or 64-oriented sections. The sample quality is dependent upon the rate of penetration (ROP). 1-in. to 2-in. resolution is typical at ROPs of 30 feet per hour[41]. The resultant high-resolution array of density or resistivity measurements is then false colored (e.g. light colors for electrically-resistive or low-density values, and dark colors for electrically-conductive or high-density values). An image log display can then be generated by unwrapping the azimuthal borehole data to generate a depth-based log of color-scaled data. In these images (e.g. in Fig. 9) the top of the borehole is found on the left and right side of the image and the quadrant positions from left to right across the image are top, right-hand side, bottom and left-hand side. The resulting real-time transmitted image is typically of sufficient quality to allow detailed wellbore stability analyses.

It should be noted, however, that when using these pseudo image logs in a quantitative way it is important to ensure that the images are corrected for distortion induced by tool eccentricity and wellbore rugosity. Also, unlike ultrasonic borehole imaging tools that make a direct measurement of the borehole surface, pseudo images based on density measurements are made at some short distance into the formation. The penetration depends upon the particular vendor's density tool configuration. Care must be exercised in interpreting bedding dips from the sinusoid amplitudes these features create in the azimuthal density log. If the measurement penetration distance is not added to the nominal borehole diameter, an error can be introduced into the prediction of the bedding dip with respect to the borehole trajectory. In smaller hole sizes this error can become significant. The separation between successive circumferential scans of the borehole along the well axis needs to be determined also, as this is influenced by the ROP. It is possible that certain artifacts may be introduced to the image by the false color interpolation between successive azimuthal scan locations.

Notwithstanding these prior caveats, Figure 18 presents an expanded view of a section from the "5-day" image of Fig. 9. The "feathery" detail on the light-colored, low-density, broken-out zone suggests a bedding influence on the location and extent of instability. This, and other images from the same well, indicates the possibility of breakout formation on the sides of the hole and the subsequent migration of this failed zone towards the 2 o'clock and 10 o'clock positions around the borehole circumference. Such information can be used in analyses of time-dependent instability of formations possessing an orthotropic strength.

Use of real-time data in wellbore stability prediction

Sonic velocity is a key input parameter in any real-time drilling operations assessment, as this is typically required for pore pressure, fracture gradient and strength predictions[35]. When using logged sonic velocities with correlations for in-situ stress, strength, modulus, etc., it is important to recognize that many of these correlations were developed from compressional wave velocity measurements made on shale samples in an orientation perpendicular to bedding. Therefore, when applying these correlations in pre-drill studies using field sonic logs one should preferably use sonic logs from vertical off-set wells.

Shales are anisotropic in their various properties. The acoustic wave velocity is not the same perpendicular to bedding as it is parallel to bedding[42,43]. The strength is not the same either, as discussed above. In shales, the acoustic velocity tends to increase as one increases the angle between the normal to bedding and the direction of the acoustic wave propagation. The acoustic wave velocity along the bedding is typically higher than the acoustic velocity perpendicular to the bedding. For this reason, care must be used when using logged velocities directly to derive properties for real-time wellbore stability analyses.

The effect of increasing velocity (or, in logging terms, a decrease in sonic transit time – the inverse of velocity) is clearly seen in Figure 19, showing data from the Niakuk field in Alaska[44]. Here the measured velocity in deviated wells is significantly faster than that measured in vertical wells. For example, at the top of the HRZ Shale (known from Fig. 10 to possess a significant strength variation with respect to bedding), the sonic transit time, D_t, is approximately 118 μs/ft (velocity = 2.58 km/s) in a vertical well; 100 μs/ft (velocity = 3.05 km/s) in a well deviated at 39° from vertical; and 83 μs/ft (velocity = 3.67 km/s) in a well deviated at 67° to vertical.

Similarly, Brandsberg-Dahl and Barkved[45] used wireline logging data from deviated wells drilled on the North Sea Valhall Field to produce a trend of velocity versus wellbore inclination (assuming the bedding angle is almost flat-lying). Their results, reproduced in Figure 20, show a ca. 19% vertical to horizontal anisotropy ratio (2500 m/sec vertically ÷ 2100 m/s horizontally = 1.19), slightly greater than that derived by Hornby et al[44].

These variations in velocity are very significant in the prediction of required mud weights in high angle wells, as rock strength has a significant impact on the prediction. Consider, for example the following strength correlation published by Horsrud[46], based on a large database of high porosity Tertiary Shales, mostly from the North Sea:

$$UCS = 111.65(304.8/D_t)^{2.93} \quad \text{.....Eq. (3)}$$

where the unconfined compressive strength, UCS, is in units of psi when the sonic transit time is in units of μs/ft.

Applying this strength correlation to the HRZ Shale velocities quoted above, a formation strength of 1800 psi is predicted for the velocity appropriate to that logged in a vertical well. This predicted strength increases to 2924 psi in the well deviated at 39°, and to 5048 psi in the well deviated at 67°! Using the correlation for friction angle published by Lal[47], the computed value increases from 26.2° in the vertical well to 34.9° in the well deviated at 67° degrees from vertical.

This almost three-fold increase in predicted unconfined compressive strength has a substantial impact on the predicted required mud weight. Using conventional mud weight prediction approaches at this depth (here, for the sake of simplicity, ignoring strength orthotropy), based on the velocity data from the vertical well, mud weights of 11.5 ppg, 12.5 ppg and 13.35 ppg are predicted for wells at 0°, 39° and 67° deviation from vertical. (At the 9000-ft. TVD depth shown in Fig. 19, S_v = 8370 psi; S_{hmin} = 6,540 psi; S_{Hmax} = 7,360 psi; and P_p = 4,905 psi).

If the corresponding logged velocities at well deviations of 39° and 67° are used to derive rock strength parameters, the predicted 'required' mud weight in the well deviated at 39° reduces to 11.3 ppg (compared to 12.5 ppg based on data from the vertical well). The predicted 'required' mud weight reduces further to 10.4 ppg when data from the 67° deviated well is used, compared to a required 13.35 ppg mud weight using data from the vertical well. This almost 3 ppg difference in predicted mud weight – arising solely from changed strength predictions using velocities from deviated wells – is substantial enough that, were these mud weights to be applied in the field, catastrophic instability would be expected in the high-angle well drilled with this low mud weight.

This discussion on velocity anisotropy is included here, as this is believed to be a significant omission in conventional wellbore stability approaches to wells drilled at high angle. The implications on mud weight prediction are profound if this effect is not recognized very early-on in well planning. It is also of great significance when planning real-time drilling operations offshore, as some form of velocity anisotropy correction is needed.

Mitigating wellbore instability in ERD wells

The biggest risk to assuring the stability of high-angle wells is considered to be anticipating the "roof collapse" type of bedding-plane failure ahead of drilling. In near-vertical well trajectories, this mode of instability is totally suppressed[25]. It is only when the well is drilled close to the bedding-parallel direction does this mode of instability become most severe[12]. In a worst case scenario, a field development might be sanctioned on the premise that high-angle wells are feasible from a central platform location (without having drilled one as part of the appraisal phase), only to find that a fissile anisotropic shale that was benign during the vertical well

appraisal phase now prevents the drilling of the extended reach wells upon which the project depends. Alternative development options – including perhaps sub-sea tiebacks in deepwater – might severely impact field economic viability.

Appropriately identifying potential problem shales possessing anisotropic strength from measurements made in vertical and modestly-deviated wells is considered to be a legitimate focus for needed research. If it were possible to make this assessment during the appraisal stage, it would strengthen the justification for taking a core within the overburden section prior to drilling unsuccessful high-angle wells.

The data of Hornby et al[44] (Fig. 19) show that formations that are additionally known to have an anisotropic strength also show pronounced velocity anisotropy. It is very possible that suitable correlations between velocity anisotropy and mechanical anisotropy can be made. These do not exist at the current time, however. But should they be found, they would be very valuable in identifying problem zones if drilled at high angle from wireline sonic measurements made in wells of modest deviation.

In the absence of robust pre-drill identification of fissile shales that would be problematic if drilled at high angle, early diagnosis of developing hole instability in real-time becomes very important. The example in Fig. 9 shows that this capability now exists, though the quality of the images transmitted in real-time currently is not as good as that collected in memory[38]. However, intelligent drill string components capable of transmitting data at rates up to 2-megabits per second have been developed and successfully tested in commercial drilling applications[48]. Conventional mud pulse telemetry used for the transmission of data from MWD and LWD tools to surface typically functions at 3 to 6 bits/sec, rising to 12 bits/sec under ideal conditions. These relatively low data rates force multiple sensors to compete for bandwidth, limiting data density and demanding complex downhole processing in order to achieve modest real-time measurement resolution. The future combination of intelligent drill-pipe with existing downhole MWD tools will enable high-quality borehole images to be sent to the surface in real-time. This is expected to result in a step-change in the ability to monitor and diagnose instability as it forms in the well.

In addition to new technology and pre-drill prediction capability, implementing good rig-site drilling practices to minimize the potential consequences of instability and stuck-pipe is vital to successfully drill challenging ERD wells. Many of the context-setting references cited in the Introduction of this paper provide good examples of these. Of the issues that would help promote smooth drilling in potentially problematic formations, the following are considered important:

BHA design: To avoid sticking the bottomhole assembly (BHA) due to the hole packing-off, the BHA should be kept as simple and as short as possible. A rotary assembly is preferred. It is recognized that this desire, from a mechanical standpoint, is in conflict often with the need to collect LWD information to either geosteer the well or to diagnose the location and nature of the instability.

Hole cleaning: Hole cleaning is difficult when large spalled cavings have fallen from the borehole. Not only must the mud rheology be adequate to transport these cavings to surface, but the pump rate may have to be increased to provide sufficient transport capability to clean the enlarged portion of the borehole. In these cases diligent real-time monitoring of pressure-while-drilling (PWD) and other drilling indicators (torque, drag and vibrations), together with appropriate changes to drilling practices, have been shown to yield improved results[49].

Recent research has investigated the relationships between breakout width as seen in borehole images (e.g. Figs. 4 and 9) and breakout depth (as measured by multi-arm calipers) to better constrain the size of failed regions of the borehole[50]. This work has revealed new insights into the geometries of enlarged boreholes in a variety of rock types in many worldwide regions (Figure 21). The deeper, narrower breakouts occurring in sandier formations may pose greater challenges to hole cleaning than the shallower, wider breakouts that form in shalier formations.

Reaming and back-reaming: It is recommended not to circulate at drilling pump rates while back-reaming, particularly if the wellbore annulus is loaded with cuttings and cavings. The risk of losses or additional borehole collapse caused by pressure surges following a pack-off needs to be minimized. When back-reaming, back-ream all the way to the previous shoe to avoid leaving a large cuttings bed in the open borehole as a result of performing a short-trip only.

Cavings monitoring & analysis: In unstable boreholes monitoring the volume of cavings being produced, analyzing their morphology, and depth-dating their likely origin from within the borehole are all recommended practices. In conjunction with real-time images, cavings analysis not only contributes to the understanding of the development of the instability but it also can help to select the appropriate remedial actions[16]. Even when no image data are available, identifying the occurrence of blocky or tabular cavings associated with bedding-related instability (e.g. Fig. 3) is very important to differentiate this mode of failure from the more classical sidewall shear failure that results in more angular cuttings. Russell et al[51] present an excellent summary of putting many of these operational issues into practice when drilling instability-prone high-angle wells on the Tullich Field in the North Sea. In a different geologic setting, Last et al[52] describe the integrated approach they adopted to evaluate and manage wellbore instability in the Cusiana Field in Colombia.

Conclusions

When planning ERD wells the following additional issues – beyond those usually addressed to assure stability in conventional wells - need to be considered in the planning phase:

- Consider the possible impact of water-depth or ground-elevation changes occurring along the ERD well path giving rise to altered or non-typical pore pressure and fracture gradient profiles. 2D or 3D predictions of pore

pressure and fracture gradient may be necessary in these instances.
- Assess the possibility of the well trajectory orientation in relation to bedding and structural dip of the formation giving rise to additional modes of instability. This is considered to be the greatest risk to planning extended reach wells.
- Design the well trajectory carefully in relationship to faults and fault crossings. Avoid crossing faults at an oblique angle that will leave the fault plane exposed for a significant distance along the well path.
- Address potential wellbore instability issues if deviating aggressively in shallow hole sections.
- Consider the potential impact of time-dependent and fatigue-cycling effects degrading the stability of the borehole once it has been drilled.

Where the borehole trajectory becomes sub-parallel to bedding (within 30°, for example) consider utilizing one of the advanced borehole stability prediction models described in this paper that account for additional failure mechanisms that are associated with formations with anisotropic strength. Testing plug samples of any recovered shales at different orientations to bedding is encouraged to better document this strength variation. Be cognizant that sonic logs taken through these formations may display velocity anisotropy also, and that velocities logged in deviated wells can differ significantly from those from vertical wells. Log data from deviated wells should be used with great caution in pre-drill planning for ERD wells.

The foregoing discussions demonstrate that the availability of borehole imaging in real-time, coupled with thorough real-time wellbore stability prediction updating, cavings monitoring, and managed borehole pressure and hole cleaning surveillance, now makes it possible to provide the necessary level of assurance in the latest and next generation of extended reach wells.

Acknowledgements

The authors thank the management of their respective companies – BP America Inc., BP plc., Rockfield Software Ltd. and GeoMechanics International Inc., for permission to publish this paper.

References

1. Judzis, A., Stoltz, D.S. and Wolfson, L. "Managing peer assists – case study of improved extended reach performance", paper SPE/IADC 52775, presented at the 1999 SPE/IADC Drilling Conference, Amsterdam, The Netherlands, 9-11 March 1999.
2. Dowson, S.L., Willson, S.M., Wolfson, L., Ramos, G.G. and Tare, U.A. "An integrated solution of extended-reach drilling problems in the Niakuk Field, Alaska: Part 1 – wellbore stability assessment", paper SPE 56563, presented at the 1999 SPE Ann. Tech. Conf. Exhib., Houston, TX, USA, 3-6 October 1999.
3. Green, M.D., Thomesen, C.R., Wolfson, L., and Bern, P.A. "An integrated solution of extended-reach drilling problems in the Niakuk Field, Alaska: Part 2 – hydraulics, cuttings transport and PWD", paper SPE 56564, presented at the 1999 SPE Ann. Tech. Conf. & Exhib., Houston, TX, USA, 3-6 October 1999.
4. Mason, C.J., BP plc., UK. *pers. comm.*
5. Schamp, J.H., Estes, B.L. and Keller, S.R. "Torque reduction techniques in ERD wells", paper IADC/SPE 98969, presented at the IADC/SPE Drilling Conference, Miami, FL, USA, 21-23 February 2006.
6. Viktorin, R.A., McDermott, J.R., Rush, R.E. and Schamp, J.H. "The next generation of Sakhalin extended-reach drilling", paper IADC/SPE 99131, presented at the IADC/SPE Drilling Conference, Miami, FL USA, 21-23 February 2006.
7. Museaus, N. "Ringhorne development : Technologies applied in extended reach drilling – successes, failures and communication risks", paper IADC/SPE 99124, presented at the IADC/SPE Drilling Conference, Miami, FL, USA, 21-23 February 2006.
8. Hjelle, A., Teige, T.G., Rolfsen, K., Hanken., K.J., Hernes, S. and Huelvan, Y. "World-record ERD well drilled from a floating installation in the North Sea", paper IADC/SPE 98945, presented at the IADC/SPE Drilling Conference, Miami, FL, USA, 21-23 February 2006.
9. Ogilvie, W., Chandler, R.B., Devlin, A., Kile, H., Rolfsen, K. and Eilertsen, Ø. "Achieving Statoil Visund's world record reach with intermediate size drill pipe – a case history", paper IADC/SPE 99172, presented at the IADC/SPE Drilling Conference, Miami, FL, USA, 21-23 February 2006.
10. Willson, S.M., Edwards, S., Heppard, P.D., Li, X., Coltrin, G., Chester, D.K., Harrison, H.L. & Cocales, B.W "Wellbore stability challenges in the deep water, Gulf of Mexico: Case history examples from the Pompano Field" paper SPE 84266, presented at the SPE Ann. Tech. Conf. & Exhib., Denver, CO, USA, 5 – 8 October 2003.
11. Rocha, L.A.S., Andrade, R. & Freire, H.L.V., "Important aspects related to the influence of water depth on ERW", paper IADC/SPE 87218, presented at the IADC/SPE Drilling Conference, Dallas, TX, USA, 2-4 March 2004.
12. Økland, D. and Cook, J. "Bedding-related instability in high-angle wells", paper SPE/ISRM 47285, presented at the SPE/ISRM Eurock'98 Conference, Trondheim, Norway, 8-10 July, 1998.
13. Bradford, I.D.R., Aldred, W.A., Cook, J.M., Elewaut, E.F.M., Fuller, J.A., Kristiansen, T.G. & Walsgrove, T.R., "When Rock mechanics met drilling: effective implementation of real-time wellbore stability control", paper SPE/IADC 59121, presented at the IADC/SPE Drilling Conference, New Orleans, LA, USA, 23-25 February 2000.
14. Beacom, L., Nicholson, H., & Corfield, R.I., "Integration of drilling and geological data to understand wellbore instability", paper SPE/IADC 67755, presented at the SPE/IADC Drilling Conference, Amsterdam, The Netherlands, 27 February-1 March 2001.
15. Davatzes, N.C. and Aydin,A., "Distribution and nature of fault architecture in a layered sandstone and shale sequence: An example from the Moab fault, Utah". In: R. Sorkhabi and Y. Tsuji, eds., Faults, fluid flow, and petroleum traps: AAPG Memoir 85, pp.153-180, 2005.
16. Edwards, S., Matsutsuyu, B. & Willson, S.M. "Real-time imaging of borehole failures", SPE Drilling & Completion Journal, Vol. 19, No. 4, December 2004, pp. 236-243.
17. Zoback, M.D., "Reservoir Geomechanics: Earth Stress and Rock Mechanics Applied to Exploration, Production and Wellbore Stability", Cambridge Press, *in press* (publ. 2007), 504 pp.
18. Barton, C.A., Zoback, M.D. and D. Moos "Fluid flow along potentially active faults in crystalline rock", Geology, v.23, no.8, pp. 683-686, 1995.
19. Fox, R.J., BP America Inc., *pers. comm.*.
20. Santos, H., Diek, A. & Roegiers, J.-C., "Wellbore stability: a new conceptual approach based on energy", paper SPE 49264, presented at the SPE Ann. Tech. Conf. & Exhib., New Orleans, LA, USA, 27-30 September 1998.

21. van Oort, et al., "Critical parameters in modeling the chemical aspects of borehole stability in shales and in designing improved water-based shale drilling fluids", paper SPE 28309, presented at the 69th SPE Ann. Tech. Conf. & Exhib., New Orleans, LA, USA, September 25-28, 1994.
22. Rojas, J.C., Clark, D.E. & Zhang, J. "Stressed shale drilling strategy – water activity design improves drilling performance", paper SPR 102498, presented at the 2006 SPE Ann. Tech. Conf. & Exhib., San Antonio, TX, USA, 9-12 October 2006.
23. Brehm, A., Ward, C., Bradford, D. & Riddle, G. "Optimizing a deepwater subsalt drilling program by evaluating anisotropic rock strength effects on wellbore stability and near-wellbore stress effects on the fracture gradient", paper IADC/SPE 98227, presented at the IADC/SPE Drilling Conference, Miami, FL, USA, 21-23 February 2006.
24. Last, N.C. and McLean, M.R. "Assessing the impact of trajectory on wells drilled in an overthrust region", paper SPE 30465, presented at the SPE Ann. Tech. Conf. & Exhib., Dallas, TX, USA, 22-25 October 1995.
25. Willson, S.M., Last, N.C., Zoback, M.D., & Moos, D.B., "Drilling in South America: a wellbore stability approach for complex geologic conditions", paper SPE 53940, presented at the 6th LACPEC Conference, Caracas, Venezuela, 21-23 April 1999.
26. Crook, A, Yu, J-G & Willson, S.M., "Development and verification of an orthotropic 3D elastoplastic material model for assessing borehole stability in shales", paper SPE/ISRM 78238, presented at the OilRock 2002 SPE/ISRM Rock Mechanics Conference, Irving TX, USA, 20-23 October 2002.
27. Niandou, H. et al. "Laboratory investigation of the mechanical behaviour of Tournemire Shale", Int. J. Rock Mech. Min. Sci., Vol.34, No.1, 3-15, 1997.
28. Ajalloeian, R. & Lashkaripour, G.R. "Strength anisotropies in mudrocks", Bull. Eng. Geol. Env. (2000) 59; 195-199.
29. Bažant, Z.P. & Oh, B., "Crack band theory for fracture of concrete", RILEM, Materials and Structures, Vol. 16, pp.155-177, 1983.
30. Jaeger, J.C., "Shear failure in anisotropic rocks", Geol. Mag., Vol..97, 65-72, 1960.
31. Jaeger, J.C. & Cook, N.G.W. "Fundamentals of Rock Mechanics", Third Edition, publ. Chapman and Hall Ltd., London, 1979.
32. Lambe, T.W. & Whitman, R.V., "Soil Mechanics, SI Version", publ. John Wiley & Sons, New York, 1979.
33. Atkinson, C., & Bradford, I., "Effect of inhomogeneous rock properties on the stability of wellbores", Proc. IUTAM Symp. on Analytical & Computational Fracture Mechanics of Non-Homogeneous Materials, Cardiff University, UK, June 18-22, 2001.
34. Malinverno, A., Sayers, C., Woodward, M.J., & Bartman, R.C., "Integrating diverse measurements to predict pore pressure with uncertainties while drilling", paper SPE 90001, presented at the SPE Ann. Tech. Conf. & Exhib., Houston, TX, USA, 26-29 September, 2004.
35. Standifird, W. and Matthews, M.D., "Real-time basin modeling: improving geopressure and earth stress predictions", paper SPE 96464, presented at the Offshore Europe 2005 Conference, Aberdeen, UK, 6-9 September 2005.
36. Greenwood, J.A., Brehm, A., van Oort, E., Algu, D,R, & Volokitin, Y.E., "Application of real-time wellbore stability monitoring on a deepwater ERD well", paper SPE/IADC 92588, presented at the SPE/IADC Drilling Conference, Amsterdam, The Netherlands, 23-25 February, 2005.
37. van Oort, E., Rosso, R., & Cabello-Montero, J., "Evolution of real-time operations monitoring: from concept to global implementation" paper SPE 97059, presented at the SPE Ann. Tech. Conf. & Exhib., Dallas, TX., USA, 9-12 October, 2005
38. Greenwood, J., Bowler, P., Sarmiento, J.F., Willson, S.M. & Edwards, S.T., "Evaluation and application of real-time image and caliper data as part of a wellbore monitoring provision", paper IADC/SPE 99111, presented at the IADC/SPE Drilling Conference, Miami, FL, 21-23 Feb., 2006.
39. Zoback, M.D. et al "Determination of stress orientation and magnitude in deep wells", Int. J. Rock Mech. & Min. Sci., 40 (2003), pp. 1049-1076.
40. Bratton, T., Bornemann, T., Li, Q., Plumb, D., Rasmus, J., & Krabbe, H., "Logging-while-drilling images for geomechanical, geological and petrophysical interpretations", paper JJJ, Transactions of the SPWLA 40th Annual Logging Symposium, Oslo, Norway, May 30 – June 3, 1999.
41. Tribe, I., Holm, G., Harker, S., Longis, C., Milne. K., Stromberg, S., Greiss, R., & Webb, K., "Optimized horizontal well placement in the Otter Field, North Sea, using new formation imaging while drilling technology", paper SPE 83968, presented at the Offshore Europe 2003 Conference, Aberdeen, UK, 2-5 September 2003.
42. Thomsen, L.A., "Weak elastic anisotropy", Geophysics, 1986, 51(6):1954-1966.
43. Hornby, B.E., "Experimental laboratory determination of the dynamic elastic properties of wet, drained shales", JGR, Vol. 103, No. B12, pp. 29,945-29,964, December 1998.
44. Hornby, B.E., Howie, J.M. & Ince, D.E. "Anisotropy correction for deviated-well sonic logs: Application to seismic well tie", Geophysics, Vol. 68, No. 2 (March – April 2003), pp. 464-471.
45. Brandsberg-Dahl, S. and Barkved, O.I. "Anisotropic P-wave velocity derived from deviated wells at the Valhall field", presented at the EAGE 64th Conference & Technical Exhibition, Florence, Italy, May 27-30, 2002.
46. Horsrud, P., "Estimating mechanical properties of shale from empirical correlations", SPE Drilling & Completion, 16, 68-73, 2001.
47. Lal, M., "Shale stability: drilling fluid interaction and shale strength", paper SPE 54356, presented at the 6th SPE LAPEC Conference, Caracas, Venezuela, 21-23 April 1999.
48. Reeves, M.E., Payne, M.L., Ismayilov, A.G., & Jellison, M.J., "Intelligent drill string field trials demonstrate technology functionality", paper SPE/IADC 92477, presented at the SPE/IADC Drilling Conference, Amsterdam, The Netherlands, 23-25 February, 2005.
49. Lapierre, S., Courville, G., & Song, J., "Achieving technical limits: expanded application of real-time pressure-while-drilling data helps optimize ROP and hole cleaning in large-diameter, directional intervals", Paper IADC/SPE 99142, presented at the IADC/SPE Drilling Conference, Miami, FL, USA, 21-23 February, 2006.
50. Moos, D.B., Willson, S.M., & Barton, C.A., "Impact of rock properties on the relationship between wellbore breakout width and depth", to be presented at the 1st Canada-U.S. Rock Mechanics Symposium, Vancouver, Canada, May 27-31, 2007.
51. Russell, K.A., Ayan, C., Hart, N.J., Rodriguez, J.M., Scholey, H., Sugden, C., & Davidson, J.K. "Predicting and preventing wellbore instability: Tullich Field Development, North Sea", paper SPE 84269, SPE Drilling & Completion Journal, Volume 21, Number 1, March 2006, pp. 12-22.
52. Last, N., Plumb, R., Harkness, R., Charlez, P., Alsen, J. & McLean, M., "An integrated approach to evaluating and managing wellbore instability in the Cusiana Field, Colombia, South America", paper SPE30464, presented at the SPE Ann. Tech. Conf. and Exhib., Dallas, TX, USA, 22-25 October, 1995.

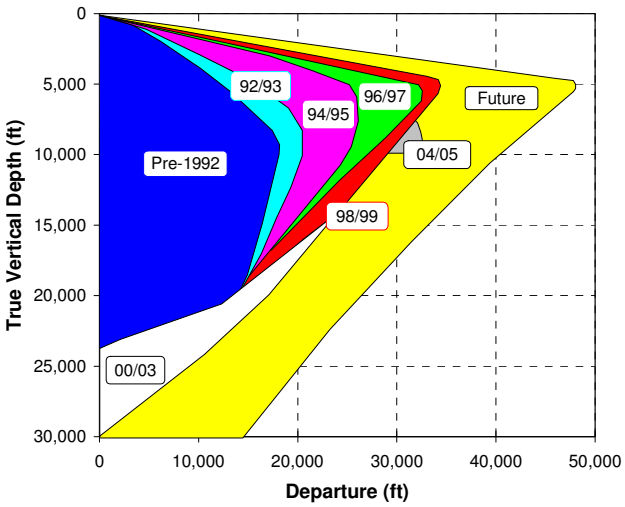

Fig. 1 – Industry ERD well evolution over time

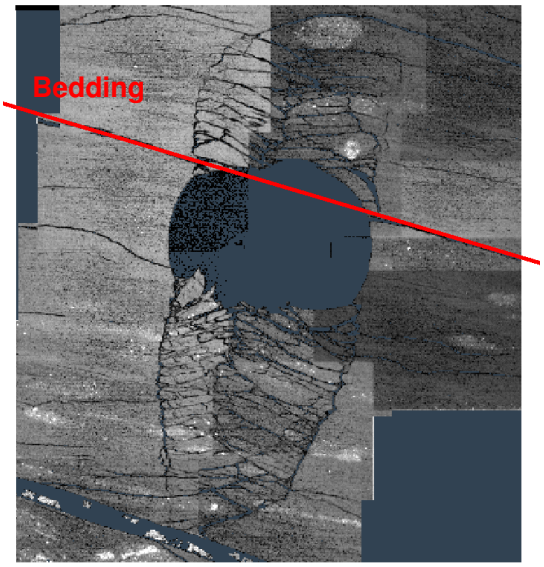

Fig. 2 – SEM photographic montage of the bedding-parallel collapse mechanism in a thick-walled cylinder test performed in Jurassic Draupne Shale with the borehole oriented parallel to bedding (from Økland & Cook[12]).

Fig. 3 – Blocky cavings recovered from extended-reach wells drilled at the Valhall field, indicative of bedding-parallel failure[13].

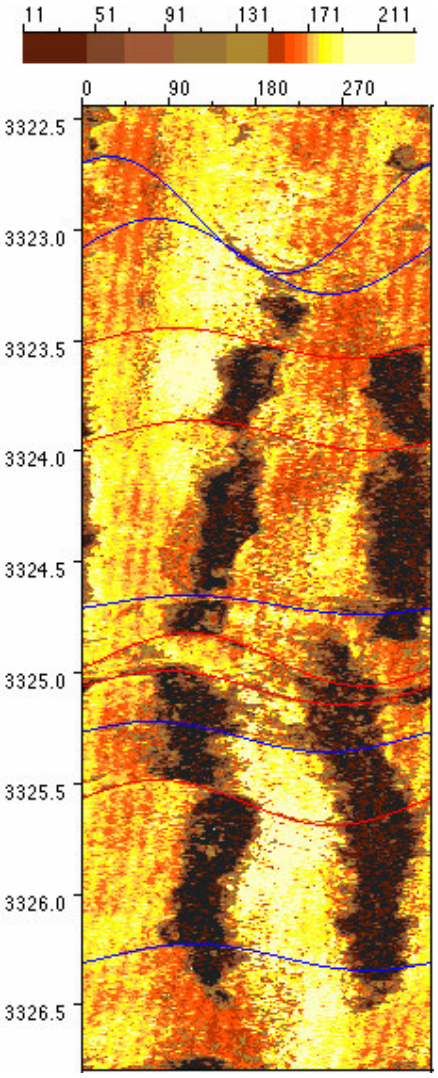

Fig. 4 – Rotation of breakouts, seen in a UBI log – indicating rotated stress states in the vicinity of a fault zone (from Zoback, 2007[17])

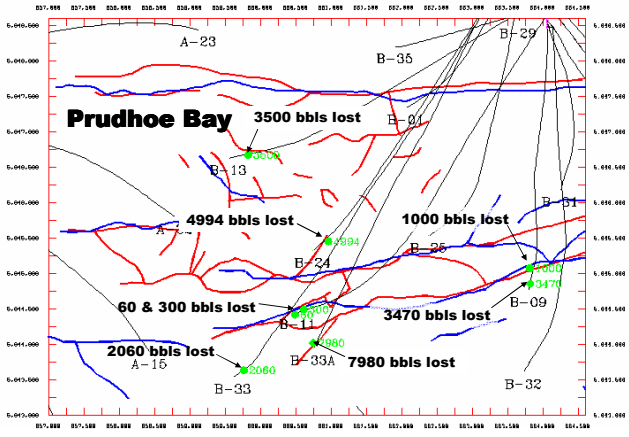

Fig. 5 – Plan view map of fault traces, well paths and occurrences of losses in the Prudhoe Bay Field, Alaska. Note the correspondence of the occurrence of losses with fault crossings.

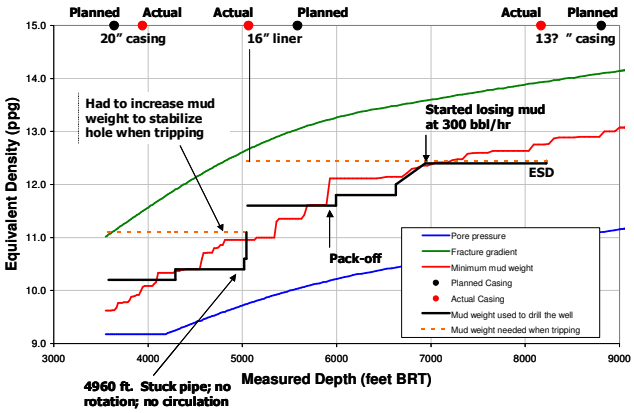

Fig. 6 – Predicted vs. 'as-drilled' mud weights in the shallow section of the TB-09 ERD well drilled from the Pompano platform[10].

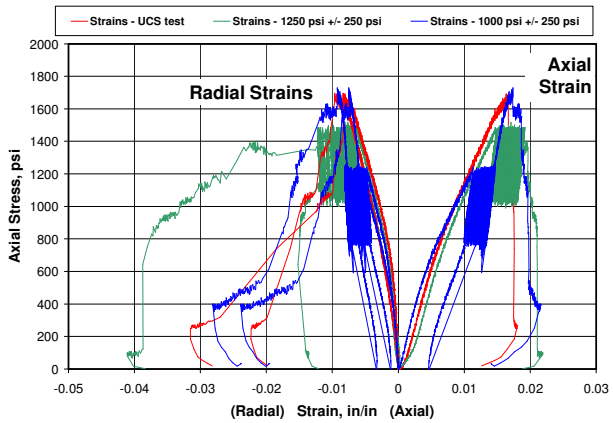

Fig 7. – Impact of stress cycling on the measured strength of Pierre I Shale.

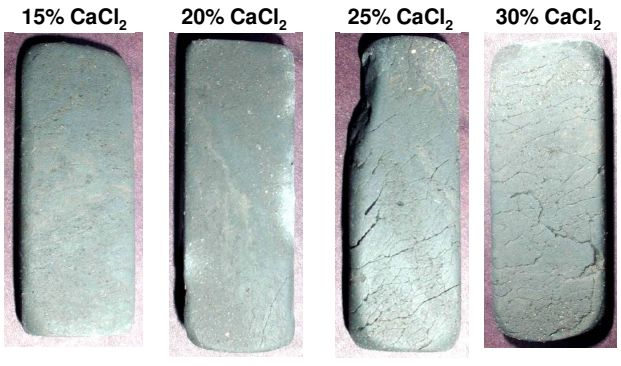

Fig. 8 - Impact on water-phase salinity on shale integrity (from[22])

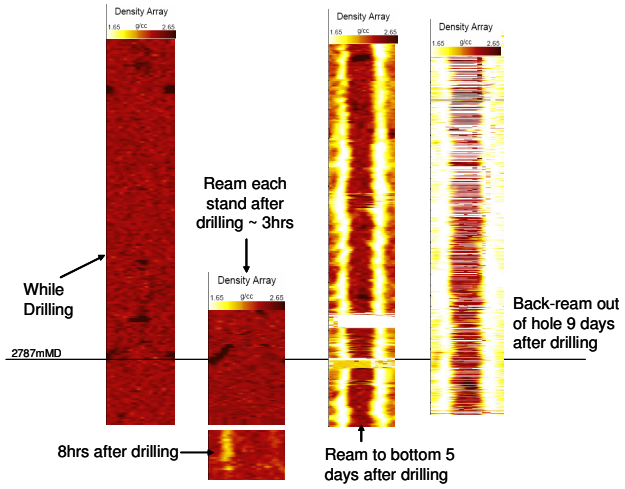

Fig 9. - Example of time-delayed instability seen from azimuthal density images in a recent North Sea ERD well.

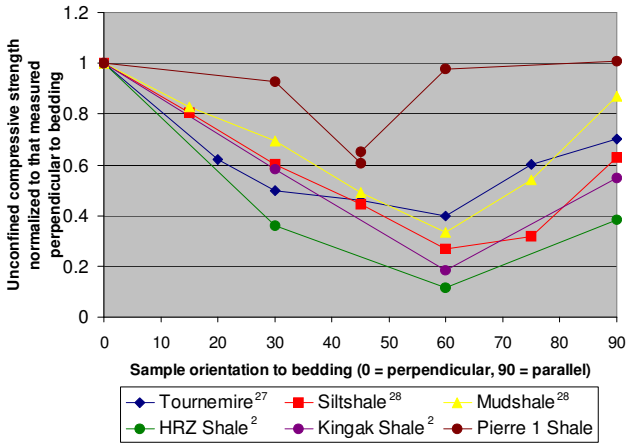

Fig. 10 – Experimental data showing strength anisotropy in shale.

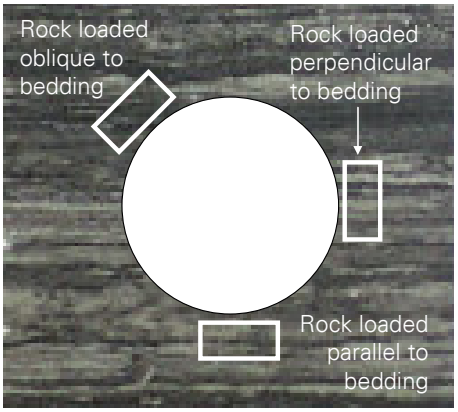

Fig. 11 – Schematic showing orientation of near-wellbore stress concentrations with respect to bedding in a horizontal wellbore.

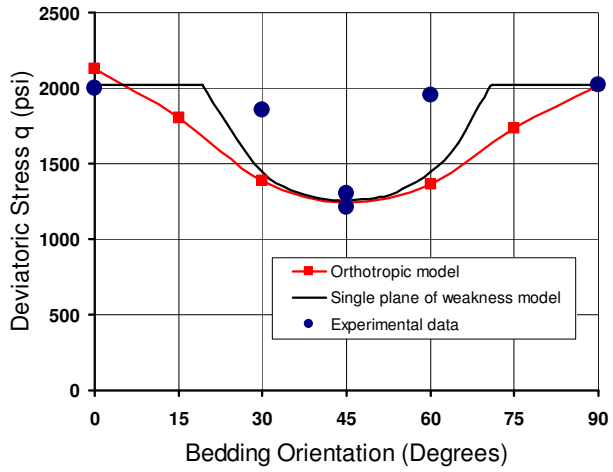

Fig. 12 – Comparison between a 'single plane of weakness' failure model and one based on orthotropic strength for Pierre I Shale.

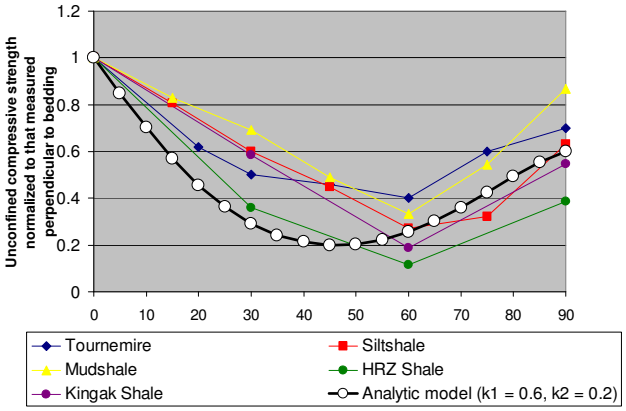

Fig. 13 - Comparison between orthotropic strength model (k_1=0.6 and k_2=0.2) and Alaska shale data[2].

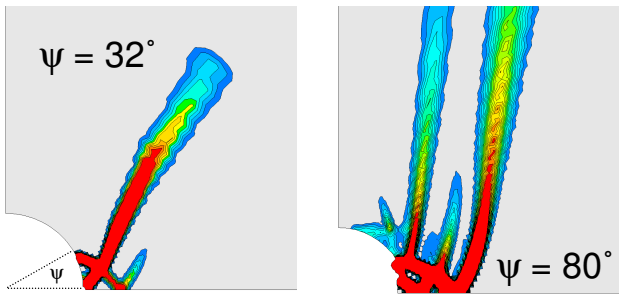

Fig. 14 - Numerical predictions of equivalent plastic strain, used here as a measure of borehole failure, around a horizontal well - isotropic and orthotropic strength representations.

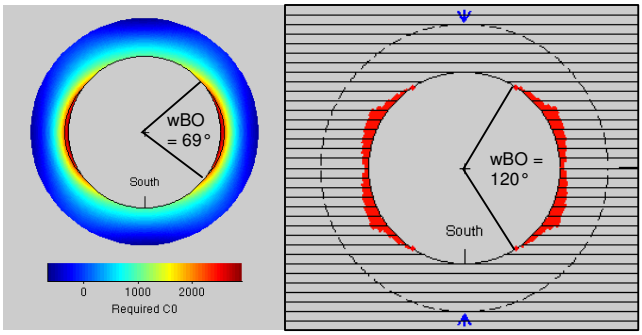

Fig. 15 – Analytical predictions of damage around a horizontal well - isotropic and orthotropic strength representations.

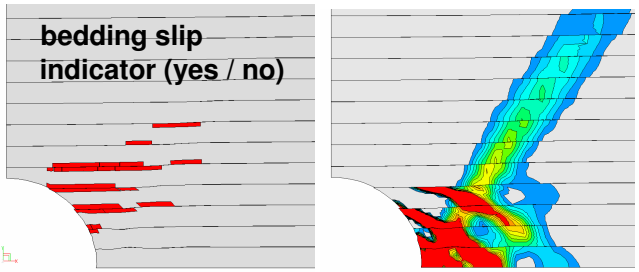

Fig. 16 - Numerical predictions of borehole failure using a discrete bedding plane model. The left-hand plot shows regions where bedding plane slip has exceeded the Mohr frictional limit of the laminae. The right-hand plot shows contours of equivalent plastic strain, used here as a measure of borehole failure.

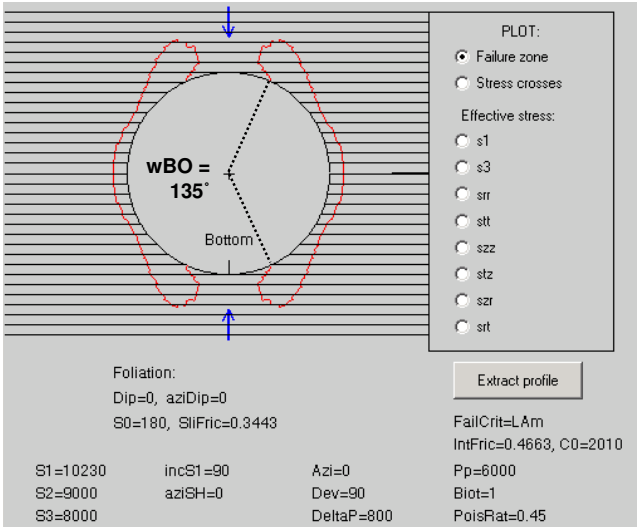

Fig. 17 – Analytical prediction of borehole failure using a single plane of weakness model. The red line delimits the extent of near-wellbore failure where the peak strength of either the intact formation or weak bedding plane is exceeded.

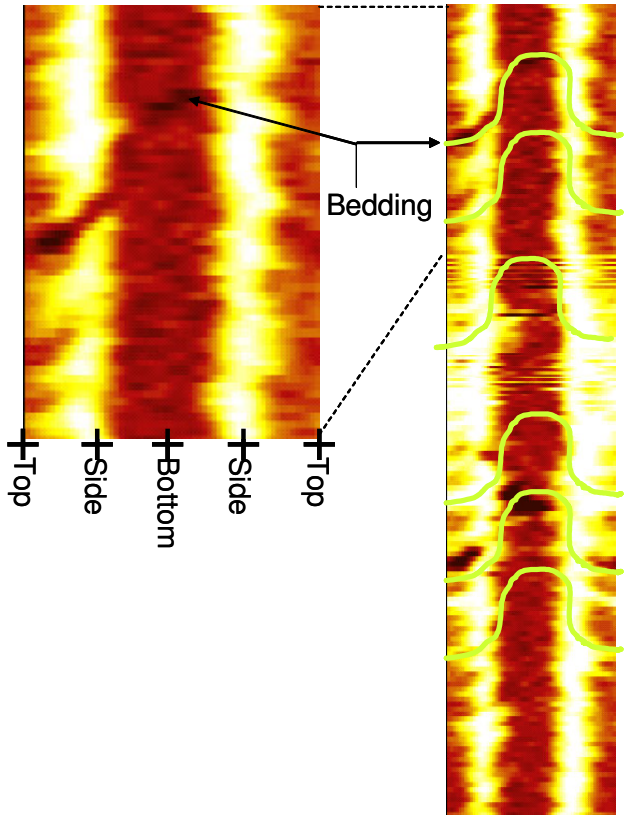

Fig. 18 – Expanded view of a LWD azimuthal density pseudo-image showing the influence of bedding features on the inferred hole enlargement (data extracted from Figure 9, 5-day view).

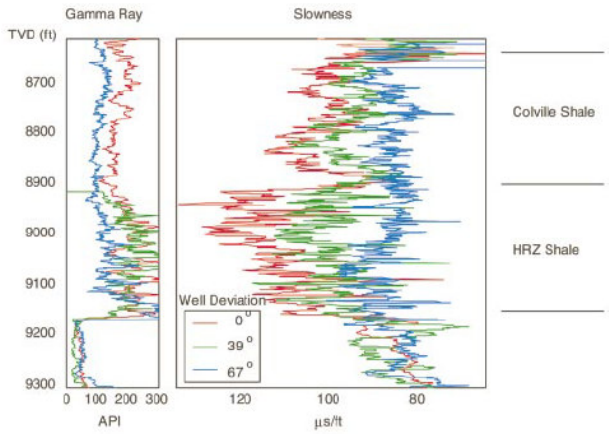

Fig. 19 - Effect of well deviation on sonic log slowness (after Hornby et al[44]). Here data from three wells are shown from the Niakuk Field: Niakuk 1A (0°), Niakuk 6 (39°) and Niakuk 14 (67°). Anisotropy is clearly evident in the HRZ and Colville shales overlying the Kuparuk reservoir.

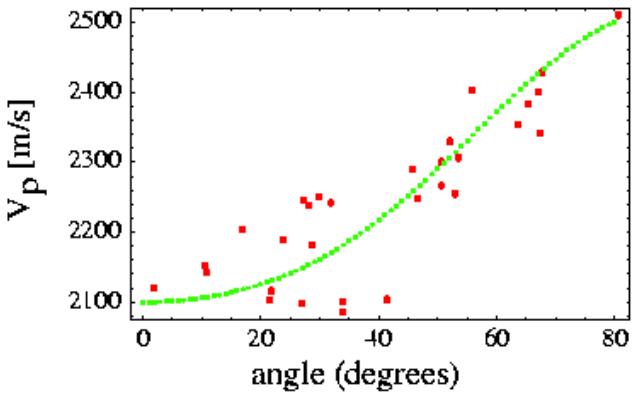

Fig. 20 - Sonic log P-wave velocity from deviated wells as a function of angle in a shale formation in the overburden (from Brandsberg-Dahl & Barkved[45]). The sonic log measurements (red dots) are taken from a large number of deviated wells. They represent both a spatial and angular sampling of the formation. The curve represents the best-fit velocity function.

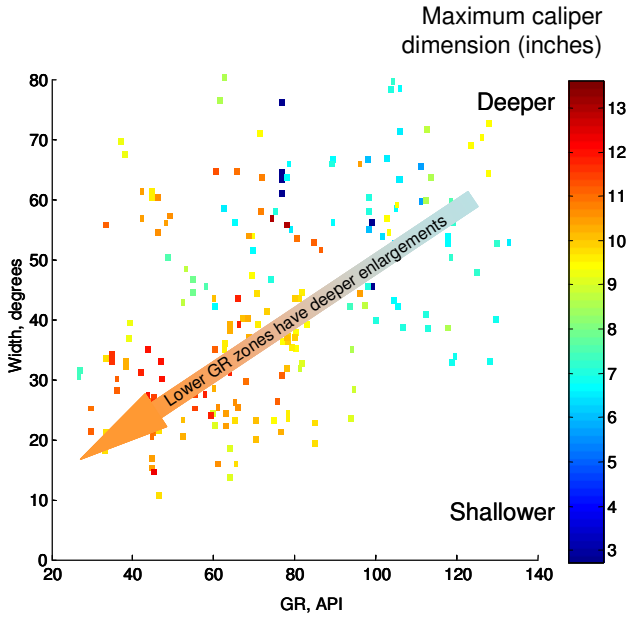

Fig. 21 – Results of an integrated study of hole enlargement, breakout size and formation type (from Moos et al[50]). Note that the sandier formations have deeper, narrower breakouts than the shallower, wider breakouts occurring in shalier material.